Report

Current Biology

Biogeography of the Global Ocean's Mesopelagic Zone

Graphical Abstract

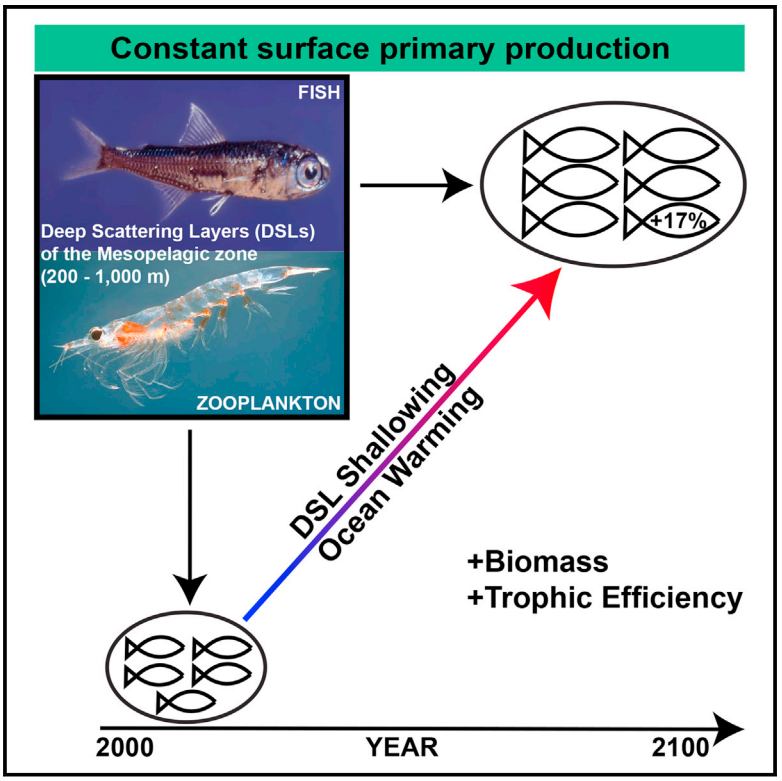

Authors

Roland Proud, Martin J. Cox, Andrew S. Brierley

Correspondence

rp43@st-andrews.ac.uk

In Brief

Proud et al. show that the global ocean can be partitioned into spatially distinct mesopelagic (200–1,000 m) provinces based on the depth of, and echo intensity from, acoustic DSLs. They reveal environmental drivers of DSL variability and infer a significant increase in mesopelagic biomass and trophic efficiency by 2100.

Highlights

- Deep scattering layer (DSL) variability demarks a global mesopelagic biogeography
- DSL backscattering intensity is predictable from primary productivity and temperature
- DSL depth is predictable from primary productivity and surface wind stress
- DSL shallowing and ocean warming will give rise to an increase in DSL biomass by 2100

Proud et al., 2017, Current Biology *27*, 113–119
January 9, 2017 © 2017 Elsevier Ltd.
http://dx.doi.org/10.1016/j.cub.2016.11.003

CellPress

Current Biology
Report

Biogeography of the Global Ocean's Mesopelagic Zone

Roland Proud,[1,3,*] Martin J. Cox,[2] and Andrew S. Brierley[1]
[1]Pelagic Ecology Research Group, Gatty Marine Laboratory, Scottish Oceans Institute, University of St Andrews, East Sands, St Andrews KY16 8LB, Scotland, UK
[2]Australian Antarctic Division, 203 Channel Highway, Kingston, TAS 7050, Australia
[3]Lead Contact
*Correspondence: rp43@st-andrews.ac.uk
http://dx.doi.org/10.1016/j.cub.2016.11.003

SUMMARY

The global ocean's near surface can be partitioned into distinct provinces on the basis of regional primary productivity and oceanography [1]. This ecological geography provides a valuable framework for understanding spatial variability in ecosystem function but has relevance only partway into the epipelagic zone (the top 200 m). The mesopelagic (200–1,000 m) makes up approximately 20% of the global ocean volume, plays important roles in biogeochemical cycling [2], and holds potentially huge fish resources [3–5]. It is, however, hidden from satellite observation, and a lack of globally consistent data has prevented development of a global-scale understanding. Acoustic deep scattering layers (DSLs) are prominent features of the mesopelagic. These vertically narrow (tens to hundreds of m) but horizontally extensive (continuous for tens to thousands of km) layers comprise fish and zooplankton and are readily detectable using echosounders. We have compiled a database of DSL characteristics globally. We show that DSL depth and acoustic backscattering intensity (a measure of biomass) can be modeled accurately using just surface primary productivity, temperature, and wind stress. Spatial variability in these environmental factors leads to a natural partition of the mesopelagic into ten distinct classes. These classes demark a more complex biogeography than the latitudinally banded schemes proposed before [6, 7]. Knowledge of how environmental factors influence the mesopelagic enables future change to be explored: we predict that by 2100 there will be widespread homogenization of mesopelagic communities and that mesopelagic biomass could increase by approximately 17%. The biomass increase requires increased trophic efficiency, which could arise because of ocean warming and DSL shallowing.

RESULTS

Deep Scattering Layers and Acoustic Sampling

Deep scattering layers (DSLs) are ubiquitous features of the global ocean that comprise biomass-rich communities of zooplankton and fish. They are so dense (biomass per unit volume) that in early acoustic surveys echoes from DSLs were mistaken for seabed echoes, hence the common name "false bottom." The mesopelagic is defined as the 200 to 1,000 m depth horizon (e.g., [8]). The physics of sound propagation enables this zone to be sampled effectively from the surface with commonly employed 38-kHz echosounders. Previous studies from tropical to sub-polar seas suggest that DSLs are rare beneath 1,000 m (e.g., [9, 10]).

General Characteristics of Regional-Scale DSLs

We used an automated, reproducible technique [11] to identify and characterize DSLs in 38-kHz acoustic data collected from the top 1,000 m by numerous research and fishing vessels around the world. We collated data from survey transects totaling 104,688 km in length (see Figure S1). Together these contained 26,474 DSLs >10 km long.

Inspection of the global DSL dataset revealed pronounced geographic differences in DSL depth, vertical extent (thickness), and acoustic backscattering intensity (quantified as area backscattering coefficient [ABC], $m^2\ m^{-2}$ [12]). ABC can be a linear proxy for biomass [3]. In this case, ABC is the total acoustic backscatter per m^2 from DSLs in the mesopelagic zone: henceforth, we use the term "backscatter" for simplicity. Although it is tempting to convert backscatter to a measure of actual biomass [3], we lack the data on species composition and size, and also on acoustic target strength, to do this [13]. Our analysis henceforth is therefore relative rather than absolute.

Generally speaking, during the daytime, the mesopelagic zone contained a principle DSL that was vertically broad (extending over >200 m vertically), relatively dense (backscatter approximately $1.59 \times 10^{-5}\ m^2\ m^{-2}$), and commonly (>66% chance) centered at a depth of approximately 525 m (Figure 1). There was also sometimes (<20% chance) a secondary, less dense DSL (backscatter approximately $1.26 \times 10^{-6}\ m^2\ m^{-2}$) approximately 300 m deeper.

Environmental Drivers of DSL Variability

Differences in DSL characteristics across oceanographic frontal boundaries have been reported previously [15], but variability at

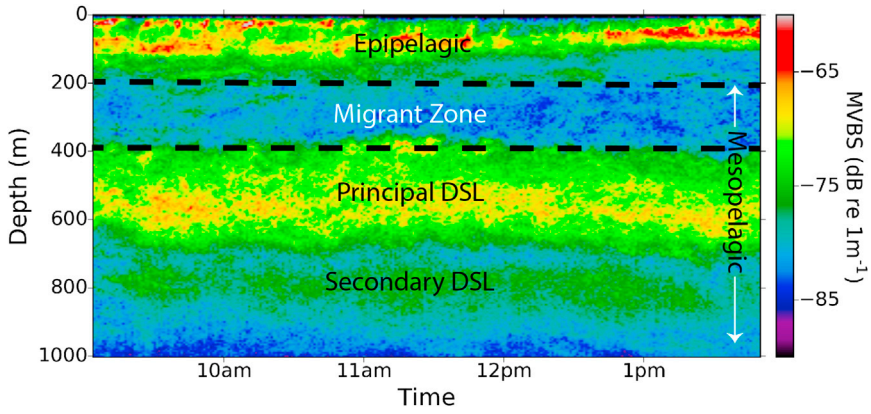

Figure 1. Scattering Layer Daytime Vertical Distribution and Acoustic Backscattering Intensity

A typical daytime water-column acoustic profile (an echogram), showing a "surface" scattering layer in the epipelagic zone (0–200 m), a principal deep scattering layer (DSL) at around 525 m (the global mean), and a secondary DSL at around 825 m, both in the mesopelagic (200–1,000 m). Data were recorded using a 38-kHz echosounder from the fishing vessel Will Watch [14] on May 30, 2012 in the southwest Indian Ocean (28.8°S, 47.3°E). The color bar is mean volume backscattering strength (MVBS, dB re 1 m^{-1}; [12]).

the global scale has not been quantified. The spatial coverage of our data spanned 14 of Longhurst's [1] 32 pelagic surface provinces (excluding his coastal biome; see Figure S1). We binned daytime DSL data by these surface provinces (there can be major differences between daytime and nighttime depths of DSLs due to diel vertical migration [16], so we separated daytime and nighttime data to avoid introducing temporal artifacts to our spatial analysis). Variability in depth of the principle daytime DSL (Z_{PDSL}, m; see Figure 1) was explained well at this spatial scale (n = 14, R^2 = 0.68, root-mean-square error [RMSE] = 28 m) by a simple multilinear model with mean annual primary production (PP, g C m^{-2} day^{-1}, p = 0.01) and surface wind stress (τ, N m^{-2}, p = 0.001) as explanatory variables (Figure 2A). The variability in backscatter from DSLs was explained well (n = 14, R^2 = 0.65, RMSE = 9.11 × 10^{-6} m^2 m^{-2}) by a simple multilinear model incorporating PP (p = 0.017) and the temperature at the depth of the principal DSL (T_{PDSL}, °C, p = 0.0001; Figure 2B).

Mesopelagic Biogeography

We used a clustering approach to explore the likely geographic distribution of distinct DSL types across the global ocean (areas where total depth ≥1,000 m). We gridded (at 300 × 300 km scale) PP and T_{PDSL} (estimated from predicted values of Z_{PDSL}, which is a function of PP and τ; see Figure 2A) and used K-means clustering (see Supplemental Information) of the normalized variables to identify coherent mesopelagic classes across a range of spatial scales (from n = 3 to 35 classes globally, classes having characteristic backscatter, PP and T_{PDSL} values; see Supplemental Information, Figure S3).

The ability to model regional variability in backscatter was best at the scale of 22 mesopelagic classes (n = 17, R^2 = 0.93, p < 0.0001, RMSE = 4.5 × 10^{-6} m^2 m^{-2}; Figure 2C). The best linear model included just one explanatory variable, PP × T_{PDSL}, which was positively correlated with backscatter. Although the 22-class scale was optimal for modeling spatial variability in backscatter, several other scales also enabled very good prediction (R^2 > 0.83; see Figures S2 and S3). As the number of classes increased, finer-scale features emerged in a progression from a simple polar and non-polar dichotomy, to biomes, to ocean gyres, to frontal features (see Figure S3). We selected the ten-class scale (R^2 = 0.87) to present mesopelagic biogeographic structure here (Figure 3; also see Table S1). Projecting at the ten-class scale produced a map of 36 spatially distinct mesopelagic provinces, a number similar to the 32 surface provinces advocated by Longhurst [1] (see Supplemental Information, Figure S2). By choosing to focus on this scale, we were able to compare Longhurst's surface biogeography and our mesopelagic biogeography: they do not overlap directly (Figure 3A).

Our ten-class mesopelagic biogeographic structure is more complex and heterogeneous than the simple latitudinal banding that pervades previous surface [6] and abyssal [7] schemes. Although the Southern Ocean is latitudinally banded in our scheme (reflecting the quasi-parallel oceanographic frontal structure in that ocean [18]), a markedly different arrangement is evident elsewhere. For example, the central tropical gyres of the north and south Pacific Ocean both cluster into the same class. Classes with high backscatter values (high mesopelagic biomass) are found across the north Atlantic and within frontal zones at mid-latitudes, with the exception of the south Pacific sector of the Southern Ocean. Classes with lower backscatter values (low mesopelagic biomass) include the polar oceans and the south Atlantic.

Present-Day Backscatter and Trophic Efficiency

We estimated total global backscatter by summing together the products of the predicted mean backscatter value (m^2 m^{-2}) and surface area of each mesopelagic class. The present-day value was 6.02 × 10^9 m^2 ± 1.4 × 10^9 m^2 (error limits from regression model RMSE value; see Figure 2C).

Biological production (the increase in biomass per unit time) is a function of biomass, temperature, and trophic level (TL) [19]. The mesopelagic community is made up of organisms operating at a range of TLs between 2 and 4. Myctophid fish (TL = 3.2; www.fishbase.org) are a major component of mesopelagic biomass [20, 21]. Zooplankton, squid, and gelatinous predators operate at TL = approximately 3, while herbivorous zooplankton reside at TL = 2. We used backscatter as a proxy for biomass, the temperature at the depth of the principle DSL, and a nominal modal trophic level of 3 to predict a value of DSL backscatter production (per m^2 per unit time) for each mesopelagic class. For each class, we determined a ratio of backscatter production to PP (TL = 1) and quantified the total amount of wet-weight primary-producer biomass required to generate one unit of backscatter (PP_{bs}, tonnes m^{-2}; see Supplemental Information). PP_{bs} serves as an inverse proxy for the trophic efficiency between TL 1 and TL 3, i.e., an increase in PP_{bs} signifies a decrease in trophic efficiency. For the present day, we estimated a global mean PP_{bs} value of 108

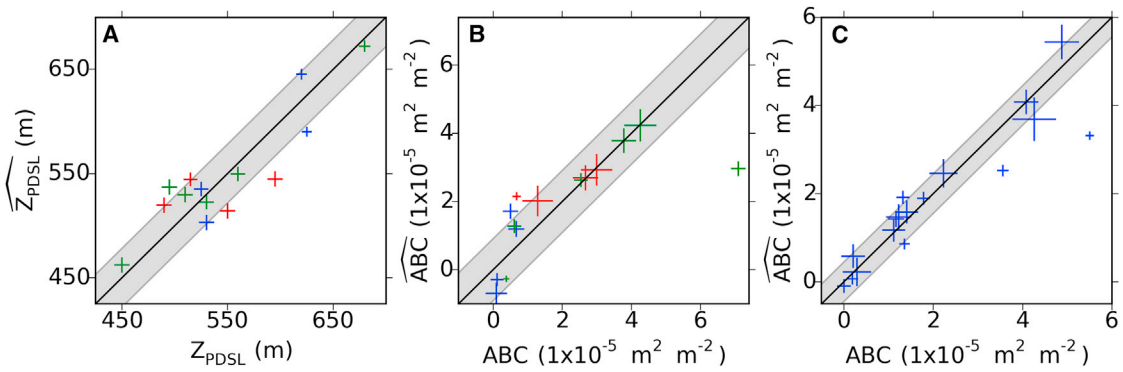

Figure 2. Weighted Linear Regressions between Observed and Predicted Principal Depths of, and Acoustic Backscattering Intensities from, DSLs

(A) Principal DSL depth (Z_{PDSL}, m; n = 14, R^2 = 0.68, RMSE = 28 m) predicted for 14 of Longhurst's 32 surface provinces [1], using mean values of primary production (PP, g C m^{-2} day^{-1}: data from http://www.science.oregonstate.edu/ocean.productivity/index.php) and wind stress (τ: output from SODA [17]) as explanatory variables ($\widehat{Z_{PDSL}} = 483.8 + 1272\times\tau - 143\times PP$).

(B) Backscatter (ABC, m^2 m^{-2}; n = 14, R^2 = 0.65, RMSE = 9.11 × 10^{-6} m^2 m^{-2}) predicted for 14 of the 32 surface provinces [1], using surface PP and the temperature at Z_{PDSL} (T_{PDSL}, °C: inferred from ocean temperature output from SODA [17]) as explanatory variables ($\widehat{ABC} = -1.18\times10^{-5} + 2.99\times10^{-5}\times PP + 3.38\times10^{-6}\times T_{PDSL}$).

(C) Backscatter (ABC, m^2 m^{-2}; n = 17, R^2 = 0.93, RMSE = 4.5 × 10^{-6} m^2 m^{-2}) predicted for 17 of the 22 mesopelagic classes (determined by K-means clustering of normalized gridded PP and T_{PDSL} values; see Figure S3G), using PP × T_{PDSL} as an explanatory variable ($\widehat{ABC} = -1.34\times10^{-6} + 8.62\times10^{-6}\times(PP\times T_{PDSL})$).

Cross size represents the relative weighting of samples. Z_{PDSL} is weighted by probability of observation, and backscatter is weighted by sample size (spatial coverage within surface province or mesopelagic class). Colors for (A) and (B) differentiate between Longhurst biomes: red = Trades; green = Westerlies; blue = Polar. Gray regions indicate the range of RMSE for each regression model. See also Figure S1.

tonnes m^{-2} (error limits 62 to 195.6 tonnes m^{-2} from regression model RMSE values). To enable regional comparisons of trophic efficiency to be made, we calculated mean PP_{bs} values for each of Longhurst's [1] surface provinces. PP_{bs}, and hence trophic efficiency, was geographically diverse (Figure 4A).

Impacts of Environmental Change on DSL Structure and Distribution

As the atmosphere warms, the ocean will warm [22], its density structure will change [23] (influencing stratification and near-surface nutrient supply [24]), surface wind intensity will change (influencing vertical mixing, stratification, and nutrient supply), and PP will change [25, 26]. Our finding that the depth of, and backscatter from, present-day DSLs are influenced by PP, temperature, and wind stress suggests that regional DSL characteristics will change too, in the future, as a result of expected environmental change. We used the coupled climate-ecosystem model NEMO-MEDUSA-2.0 [27] (under the Representative Concentration Pathways [RCP] 8.5 climate scenario, and with surface forcing as per the UK Meteorological Office's HadGEM2-ES model) to obtain PP, τ, and T_{PDSL} for the period 2090–2100. Values of PP and T_{PDSL} (estimated from predicted values of Z_{PDSL}, which is a function of PP and τ) were gridded (300 × 300 km scale), and each grid cell was attributed a DSL class using the K-means centroids (see Table S1) from the present-day (2005–2008) ten-class scale mesopelagic biogeography (Figure 3B).

According to NEMO-MEDUSA-2.0, oceanic PP will remain fairly constant over the 21st century, with mean values over the pelagic realm of 0.319 and 0.324 g C m^{-2} day^{-1} for the present and 2100, respectively. While there are differences between the predictions of various Earth system models, predictions of future PP by NEMO-MEDUSA-2.0 are consistent with those from a number of other models [28–31], and this ensemble agreement is mutually supportive. By 2100, the predicted mean Z_{PDSL} will be shallower on average than present (shallowing from 545 m to 510 m, RMSE = 28 m; see Figures 2A and 4B), the predicted T_{PDSL} will increase (from a mean of 7.2°C ± 0.28°C to 8.5°C ± 0.37°C, error limits based on Z_{PDSL} regression model RMSE value), and wind stress will weaken (from 0.085 to 0.058 Nm^{-2}).

Future Backscatter and Trophic Efficiency

In light of the environmental changes predicted by NEMO-MEDUSA-2.0, we estimated that global DSL backscatter will increase by 16.7% from a present-day value of 6.02 × 10^9 m^2 ± 1.4 × 10^9 to 7.03 × 10^9 m^2 ± 1.4 × 10^9 in 2100 (error limits from regression model RMSE value; see Figure 2C). We estimate that the global mean PP_{bs} will decrease from 108.0 tonnes m^{-2} (error limits from 62.0 to 195.6) to 73.9 tonnes m^{-2} (error limits from 53.6 to 145.7) by 2100 (error limits from regression model RMSE values; Figure 4A), i.e., that 34.1 tonnes less primary-producer biomass per m^2 will be needed to generate one unit of DSL backscatter by 2100, equivalent to a factor increase in trophic efficiency of 1.232 ± 0.015 (error limits from regression model RMSE values; see Supplemental Information). The predicted increase in global backscatter and decrease in the mean global value of PP_{bs} is indicative of an overall future increase in mesopelagic biomass and trophic efficiency.

DISCUSSION

The analysis reported here is the first to apply a consistent, automated technique to identify and determine characteristics of DSLs from data collected on multiple acoustic surveys across the global ocean. As such, it provides the first consistent view of DSL variability globally and has enabled the development, for the first time, of a DSL-based mesopelagic biogeography.

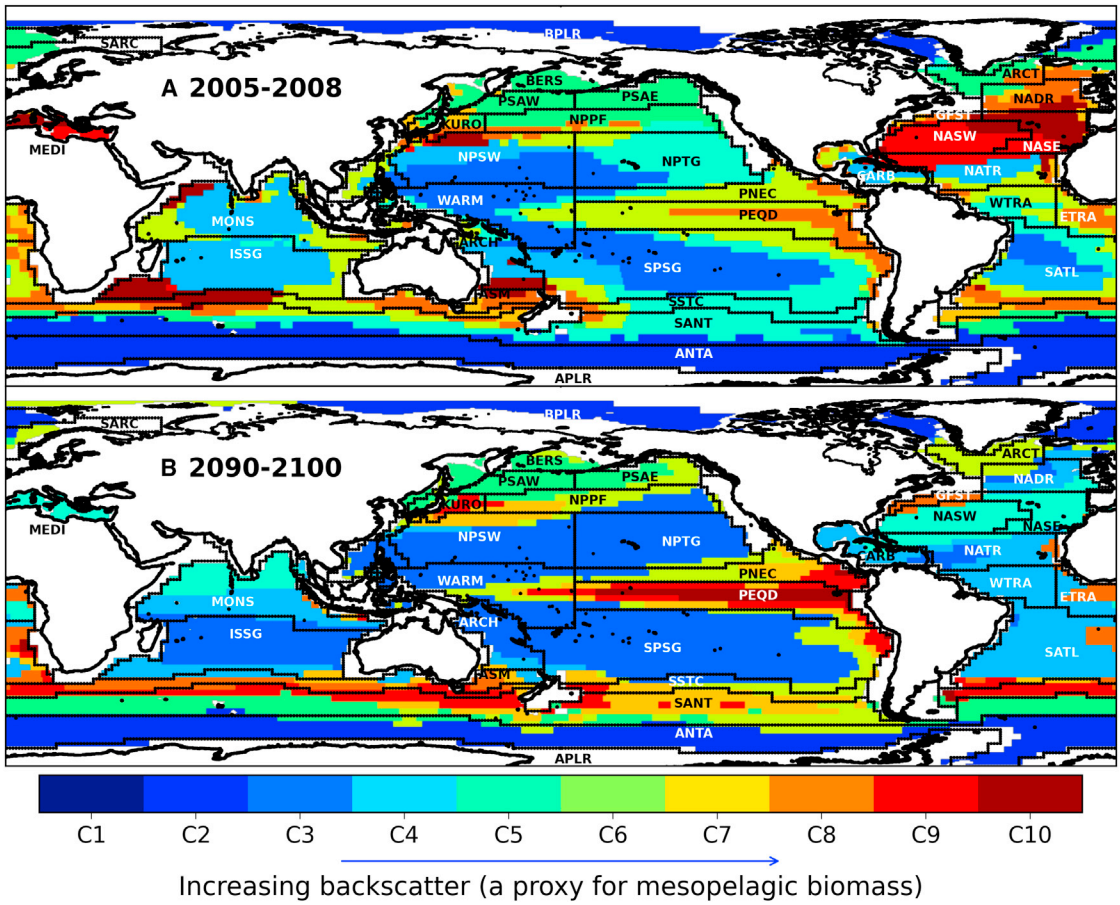

Figure 3. Present-Day Mesopelagic Biogeography Derived from Values of Surface Primary Productivity and Temperature at the Depth of the Principal DSL, and Predicted Biogeography for the Period 2090–2100

(A) Present-day mesopelagic biogeography derived by K-means clustering of gridded PP (g C m^{-2} day^{-1}: data from http://www.science.oregonstate.edu/ocean.productivity/index.php) and T_{PDSL} (°C: estimated from predicted values of Z_{PDSL} using data output from SODA [17]) values into ten classes (see Table S1 for mean values).

(B) Future mesopelagic biogeography. Gridded cells attributed to their future appropriate class using centroids from the present-day result.

Longhurst surface provinces [1] are overlaid and labeled. Each mesopelagic biogeography is formed of ten classes (that form distinct mesopelagic provinces when resolved spatially), which are ranked in order (from C1 to C10) of increasing backscatter values (proxies for mesopelagic biomass). See also Figures S2 and S3 and Table S1.

Several site-specific DSL studies have been published [32, 33], but quantitative comparisons between studies have not usually been possible because a consistent approach to DSL detection and parameterization has not been used. Longhurst's surface biogeography [1], defined in part using globally consistent satellite remote sensing data, has been extremely valuable for improving understanding of spatial variability in ecosystem function in the visible and accessible ocean surface. We hope that the analysis presented here will be of value for understanding operation on a global-scale of the ecosystem of the hidden mesopelagic realm.

Drivers of Backscatter from DSLs

Primary Production

Food web theory holds that biomass at higher trophic levels (such as zooplankton grazers at level 2 and myctophid fish predators at level 3.2) is constrained by PP [34]. Indeed PP-to-biomass relationships have already been reported for mesopelagic fish [3]. It is no surprise, therefore, that PP is a significant factor in our model of DSL backscatter (a proxy for biomass; $p = 0.01$). PP in turn is influenced by light intensity, nutrient availability, stratification and mixing, and sea-surface temperature (PP occurs in the illuminated, near-surface zone where biological processes are strongly influenced by sea-surface temperature).

Temperature at the Depth of the DSL

Sea-surface temperature was not a significant driver of backscatter ($n = 14$, $R^2 = 0.07$, $p = 0.19$), but temperature at the depth of the DSL was. Mesopelagic organisms live their lives away from the surface, which is one reason why the mesopelagic biogeography revealed here does not map well onto Longhurst's [1] surface scheme (Figure 3). Biomass, production, and production-to-biomass ratios for marine fish all vary with temperature [34] (positively; temperature influences metabolic rates and therefore growth and reproduction), and our finding of a highly significant positive linear relationship ($p = 0.0001$) between DSL backscatter and temperature at the depth of the DSL is

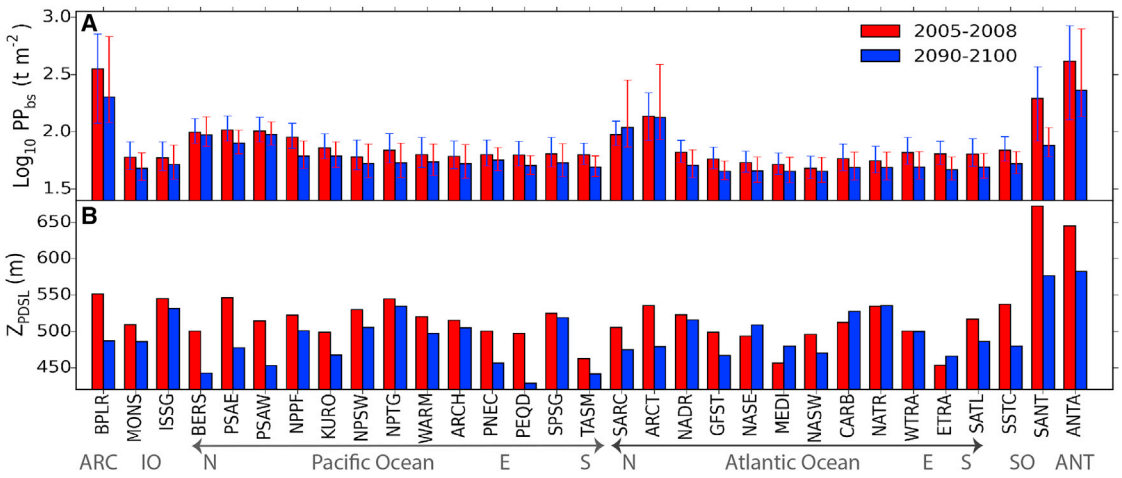

Figure 4. Global Change in PP_{bs}, an Inverse Proxy of Trophic Efficiency, and Principal DSL Depth for Each Longhurst Surface Province for the Present-Day and Future, Assuming Future Conditions as per Data Output from NEMO-MEDUSA-2.0 for the Period 2090-2100

(A) PP_{bs} (tonnes m^{-2}; primary-producer biomass required to generate one unit of backscatter per m^2 from DSLs in the mesopelagic) calculated by surface province (see Supplemental Information). Error bars are from regression model RMSE values.

(B) Predicted variability in the depth of the principle daytime DSL ($\widehat{Z_{PDSL}} = 483.8 + 1272 \times \tau - 143 \times PP$, RMSE = 28 m), where PP (g C m^{-2} day^{-1}) is primary production (data from http://www.science.oregonstate.edu/ocean.productivity/index.php) and τ (N m^{-2}) is wind stress, taken from SODA [17]. See also Figure S1.

Surface provinces are grouped by ocean and shown in latitude order from north to south: ARC is the Arctic Ocean, IO is the Indian Ocean, SO is the Southern Ocean, and ANT represents the region of the SO south of the Antarctic Polar Front. For the Pacific and Atlantic Oceans, provinces that are furthest north (N), south (S), and those that reside closest to the equator (E) are indicated.

consistent with this. A consequence is that by 2100, the majority of surface provinces where DSLs are predicted to shallow significantly (>28 m) will have increased biomasses because they will be warmer habitats (Figures 3 and 4B).

Biogeographic Change by 2100

Using predicted values of PP, τ, and T_{PDSL} for 2090–2100 (from NEMO-MEDUSA-2.0 [27]) and mapping the ten present-day mesopelagic classes onto grid cells (300 × 300 km), it becomes apparent that environmental change will lead to a marked change in global mesopelagic biogeographic structure by the end of this century (Figure 3). Prominent changes by 2100 include the low biomass regions of the north and south Pacific gyres expanding to almost fill their respective ocean basins (being separated by only a narrower, but more productive, east Equatorial Zone); the south Indian Ocean gyre decreasing in biomass (Figure 3); southern mid-latitudinal frontal zones increasing in area and biomass; the presently diverse south and central Atlantic Ocean coalescing to a more homogeneous, and relatively productive (for an open-ocean gyre system) regime, and increasing biomass in sub-polar regions. This latter change will be mediated strongly by DSL shallowing (Figure 4B) and may indicate northward and southward range expansions of mesopelagic fish. For the northern hemisphere, this in turn may be supportive of the view that the Atlantic and Arctic food webs will merge [27] and will lead to increasing abundance and diversity of polar mesopelagic fish.

Trophic Efficiency Now and by 2100

The rule of thumb mean figure for trophic efficiency is approximately 10% per trophic level [35]. As temperature increases (up to the point that it becomes physiologically challenging), for a given food supply, fish production will increase [19], yielding a higher trophic efficiency. This is because with increased temperature, more food can be metabolized per unit time, increasing growth and reproduction rates (via shorter generation times). More rapid growth also leads to increased survival and recruitment because, by growing, individuals more rapidly escape some predation risk in size-structured food webs. We predict a mean increase in trophic efficiency between trophic level 1 and 3 by a factor of 1.232 ± 0.015 by 2100. In the context of the rule of thumb 10% efficiency per trophic level, this is an increase of 1.1% per level. The magnitude and direction of change will, however, be geographically diverse because of geographic variation in temperature change and PP (food supply). At the ocean scale, the backscatter in the Atlantic as a whole is predicted to change dramatically by 2100: substantial reductions in PP (−21% caused by stratification and nutrient depletion [27]) will lead to reduced biomass (Figure 3) despite the Atlantic maintaining some of the lowest values of PP_{bs} (i.e., highest values of trophic efficiency; Figure 4A). Estimated values of PP_{bs} are presently highest in the polar regions but, by 2100, we predict substantially greater trophic efficiency in those regions due to ocean warming and DSL shallowing (Figures 3 and 4A).

Mesopelagic Fish

Although we do not know the extent to which mesopelagic fish contribute to DSL biomass [13], it is not unreasonable to expect it to be high [3]. Consequently, in light of predictions here of an increase in global backscatter by 2100 (of 16.7%), we predict an increase in the biomass of mesopelagic fish in the future.

Mesopelagic fish are a key component of pelagic food webs [36], fueling some commercially important fisheries [21]. They also play a major role in the biological pump [2, 37, 38], the active

transport of carbon to the ocean interior that buffers atmospheric CO_2, and so provide an important "ecosystem service." In recognition of these roles, the US National Oceanic and Atmospheric Administration's National Marine Fisheries Service prohibited in April 2016 commercial fisheries for myctophids (Myctophidae, or "Lantern fish" are major constituents of mesopelagic biomass) and other small forage fish in the Pacific Ocean off the US West Coast [39]. Our global-scale analysis can contribute toward ecosystem-based management of the mesopelagic because it highlights regions of relatively high (and low) biomass and because present-day spatial variability (e.g., DSL characteristics in the sub-tropics versus in temperate regions) can be used as a proxy for future temporal change (e.g., regional warming). The ability to predict the redistribution of oceanic mesopelagic production could aid conservation management by, for example, guiding placement of open-ocean marine protected areas.

Concluding Remarks

We have defined a global biogeography for the mesopelagic zone and used it to infer changes in mesopelagic biomass and trophic efficiency into the future. This has gone some way to fill the "dark hole" [4, 5] in our understanding of the mesopelagic. Predictions based on output from NEMO-MEDUSA-2.0 suggest that the mesopelagic will become more productive by 2100 but that this production will be condensed into smaller regions (e.g., concentrated at fronts) and spread poleward as DSLs shallow and the ocean warms. It has been suggested that constancy of light regime under climate change will prevent myctophid fish invading the Arctic [40]. Our results bring this into question: ice loss will bring change to the Arctic surface and—we suggest—will presage change to the deep sea there as well. These changes may bring new opportunities for fishing.

SUPPLEMENTAL INFORMATION

Supplemental Information includes Supplemental Experimental Procedures, three figures, and one table and can be found with this article online at http://dx.doi.org/10.1016/j.cub.2016.11.003.

AUTHOR CONTRIBUTIONS

A.S.B. conceived the study. R.P., A.S.B., and M.J.C. conceived the method. R.P. put the method into practice, collated the data, and analyzed the results. R.P. and A.S.B. wrote the manuscript. A.S.B., R.P., and M.J.C. edited the manuscript.

ACKNOWLEDGMENTS

We thank the British Antarctic Survey, the British Oceanographic Data Centre, the Australian Integrated Marine Observing System, and Dr. Phil Hosegood for providing echosounder data. We also thank Dr. Andrew Yool for providing output from NEMO-MEDUSA-2.0, and Dr. Mark Costello and Dr. Witold Fraczek for discussion of mesopelagic volume. This study has received support from the European H2020 International Cooperation project MESOPP (Mesopelagic Southern Ocean Prey and Predators; http://www.mesopp.eu/).

Received: June 23, 2016
Revised: October 24, 2016
Accepted: November 1, 2016
Published: December 22, 2016

REFERENCES

1. Longhurst, A.R. (2007). Ecological Geography of the Sea, Second Edition (Academic Press).
2. Davison, P.C., Checkley, D.M., Jr., Koslow, J.A., and Barlow, J. (2013). Carbon export mediated by mesopelagic fishes in the northeast Pacific Ocean. Prog. Oceanogr. *116*, 14–30.
3. Irigoien, X., Klevjer, T.A., Røstad, A., Martinez, U., Boyra, G., Acuña, J.L., Bode, A., Echevarria, F., Gonzalez-Gordillo, J.I., Hernandez-Leon, S., et al. (2014). Large mesopelagic fishes biomass and trophic efficiency in the open ocean. Nat. Commun. *5*, 3271.
4. St. John, M.A., Borja, A., Chust, G., Heath, M., Grigorov, I., Mariani, P., Martin, A.P., and Santos, R.S. (2016). A dark hole in our understanding of marine ecosystems and their services: perspectives from the mesopelagic community. Front. Mar. Sci. *3*, 1–6.
5. Webb, T.J., Vanden Berghe, E., and O'Dor, R. (2010). Biodiversity's big wet secret: the global distribution of marine biological records reveals chronic under-exploration of the deep pelagic ocean. PLoS ONE *5*, e10223.
6. Fay, A.R., and McKinley, G.A. (2014). Global open-ocean biomes: mean and temporal variability. Earth Syst. Sci. Data *6*, 273–284.
7. UNESCO (2009). Global open oceans and deep seabed (GOODS) – biogeographic classification. Paris, UNESCO-IOC. (IOC Tech. Ser. 84.). http://unesdoc.unesco.org/images/0018/001824/182451e.pdf.
8. Kaiser, M.J., Attrill, M.J., Jennings, S., Thomas, D.N., Barnes, D.K.A., Brierley, A.S., Hiddink, J.G., Kaartokallio, H., Polunin, N.V.C., and Raffaelli, D.G. (2011). Marine ecology: processes, systems, and impacts (Oxford University Press).
9. Magnússon, J. (1996). The deep scattering layers in the Irminger Sea. J. Fish Biol. *49*, 182–191.
10. Benoit-Bird, K.J., and Au, W.W.L. (2004). Diel migration dynamics of an island-associated sound-scattering layer. Deep Sea Res. Part I Oceanogr. Res. Pap. *51*, 707–719.
11. Proud, R., Cox, M.J., Wotherspoon, S., and Brierley, A.S. (2015). A method for identifying Sound Scattering Layers and extracting key characteristics. Methods Ecol. Evol. *6*, 1190–1198.
12. Maclennan, D.N., Fernandes, P.G., and Dalen, J. (2002). A consistent approach to definitions and symbols in fisheries acoustics. ICES J. Mar. Sci. *59*, 365–369.
13. Davison, P.C., Koslow, J.A., and Kloser, R.J. (2015). Acoustic biomass estimation of mesopelagic fish: backscattering from individuals, populations, and communities. ICES J. Mar. Sci. *72*, 1413–1424.
14. IMOS (2013). IMOS BASOOP sub facility. imos.org.au.
15. Boersch-Supan, P.H., Boehme, L., Read, J.F., Rogers, A.D., and Brierley, A.S. (2012). Elephant seal foraging dives track prey distribution, not temperature: comment on McIntyre et al. (2011). Mar. Ecol. Prog. Ser. *461*, 293–298.
16. Brierley, A.S. (2014). Diel vertical migration. Curr. Biol. *24*, R1074–R1076.
17. Carton, J.A., Chepurin, G., and Cao, X. (2000). A simple ocean data assimilation analysis of the global upper ocean 1950–95. Part II: results. J. Phys. Oceanogr. *30*, 311–326.
18. Orsi, A.H., Whitworth, T., and Nowlin, W.D. (1995). On the meridional extent and fronts of the Antarctic Circumpolar. Current. Deep Sea Res. I *42*, 641–673.
19. Gascuel, D., Morissette, L., Palomares, M.L.D., and Christensen, V. (2008). Trophic flow kinetics in marine ecosystems: toward a theoretical approach to ecosystem functioning. Ecol. Modell. *217*, 33–47.
20. Barham, E.G. (1966). Deep scattering layer migration and composition: observations from a diving saucer. Science *151*, 1399–1403.
21. Catul, V., Gauns, M., and Karuppasamy, P.K. (2011). A review on mesopelagic fishes belonging to family Myctophidae. Rev. Fish Biol. Fish. *21*, 339–354.

22. Abraham, J.P., and Baringer, M. (2013). A review of global ocean temperature observations: Implications for ocean heat content estimates and climate change. Rev. Geophys. *51*, 450–483.

23. Srokosz, M.A., and Bryden, H.L. (2015). Ocean Circulation. Observing the Atlantic meridional overturning circulation yields a decade of inevitable surprises. Science *348*, 1255575.

24. Behrenfeld, M.J., O'Malley, R.T., Siegel, D.A., McClain, C.R., Sarmiento, J.L., Feldman, G.C., Milligan, A.J., Falkowski, P.G., Letelier, R.M., and Boss, E.S. (2006). Climate-driven trends in contemporary ocean productivity. Nature *444*, 752–755.

25. Denman, K.L., and Gargett, A.E. (1983). Time and space scales of vertical mixing and advection of phytoplankton in the upper ocean. Limnol. Oceanogr. *28*, 801–815.

26. Laufkötter, C., Vogt, M., and Gruber, N. (2013). Long-term trends in ocean plankton production and particle export between 1960-2006. Biogeosciences *10*, 7373–7393.

27. Yool, A., Popova, E.E., Coward, A.C., Bernie, D., and Anderson, T.R. (2013). Climate change and ocean acidification impacts on lower trophic levels and the export of organic carbon to the deep ocean. Biogeosciences *10*, 5831–5854.

28. Cox, P.M., Betts, R.A., Jones, C.D., Spall, S.A., and Totterdell, I.J. (2000). Acceleration of global warming due to carbon-cycle feedbacks in a coupled climate model. Nature *408*, 184–187.

29. Bopp, L., Monfray, P., Aumont, O., Dufresne, J.L., Le Treut, H., Madec, G., Terray, L., and Orr, J.C. (2001). Potential impact of climate change on marine export production. Global Biogeochem. Cycles *15*, 81–99.

30. Bopp, L., Aumont, O., Cadule, P., Alvain, S., and Gehlen, M. (2005). Response of diatoms distribution to global warming and potential implications: a global model study. Geophys. Res. Lett. *32*, L19606.

31. Steinacher, M., Joos, F., Frölicher, T.L., Bopp, L., Cadule, P., Doney, S.C., Gehlen, M., Schneider, B., and Segschneider, J. (2010). Projected 21st century decrease in marine productivity: a multi-model analysis. Biogeosciences *6*, 7933–7981.

32. Netburn, A.N., and Anthony Koslow, J. (2015). Dissolved oxygen as a constraint on daytime deep scattering layer depth in the southern California current ecosystem. Deep Sea Res. Part I Oceanogr. Res. Pap. *104*, 149–158.

33. Fennell, S., and Rose, G. (2015). Oceanographic influences on deep scattering layers across the North Atlantic. Deep Sea Res. Part I Oceanogr. Res. Pap. *105*, 132–141.

34. Jennings, S., Mélin, F., Blanchard, J.L., Forster, R.M., Dulvy, N.K., and Wilson, R.W. (2008). Global-scale predictions of community and ecosystem properties from simple ecological theory. Proc. Biol. Sci. *275*, 1375–1383.

35. Pauly, D., and Christensen, V. (1995). Primary production required to sustain global fisheries. Nature *374*, 255–257.

36. Kawaguchi, K., and Gjoseter, J. (1980). A review of the world resources of mesopelagic fish. FAO Fisheries Technical Paper 193, FAO Rome.

37. Radchenko, V.I. (2007). Mesopelagic fish community supplies "biological pump." Raffles Bull. Zool. *2014*, 265–271.

38. Davison, P.C. (2011). The export of carbon mediated by mesopelagic fishes in the Northeast Pacific Ocean. PhD thesis (University of California, San Diego).

39. Pacific Fishery Management Council (2016). Coastal pelagic species fishery management plan, as amended through amendment 15. http://www.pcouncil.org/wp-content/uploads/2016/05/CPS_FMP_Amended_by_FinalAmendment15_amendatory_language.pdf.

40. Kaartvedt, S. (2008). Photoperiod may constrain the effect of global warming in arctic marine systems. J. Plankton Res. *30*, 1203–1206.